

PRESSURE MEASUREMENTS IN WATER-MODERATOR CROSSOVER
REGION OF TUNGSTEN WATER-MODERATED REACTOR

By Colin Heath

Lewis Research Center
Cleveland, Ohio

~~RESTRICTED DATA~~

ATOMIC ENERGY ACT OF 1954

~~GROUP 1
Excluded from automatic
downgrading and declassification~~

CLASSIFIED DOCUMENT—TITLE UNCLASSIFIED

This material contains information affecting the national defense of the United States within the meaning of the espionage laws, Title 18, U.S.C., Secs. 793 and 794, the transmission or revelation of which in any manner to an unauthorized person is prohibited by law.


NOTICE

This document should not be returned after it has satisfied your requirements. It may be disposed of in accordance with your local security regulations or the appropriate provisions of the Industrial Security Manual for Safe-Guarding Classified Information.

NATIONAL AERONAUTICS AND SPACE ADMINISTRATION

(6)

[REDACTED]



PRESSURE MEASUREMENTS IN WATER-MODERATOR CROSSOVER REGION OF TUNGSTEN WATER-MODERATED REACTOR (U)

by Colin Heath
Lewis Research Center

SUMMARY

The tube sheet of the exit-crossover plenum for the water moderator in the tungsten water-moderated rocket reactor must be thermally protected from hot propellant gases in the rocket nozzle. Preliminary thermal analysis has indicated that the governing process in cooling this plenum is the heat transfer from the exit tube sheet to the water in the plenum.


The water flow profiles inside the exit-crossover plenum were investigated. A set of characteristic curves was experimentally obtained for circumferential pressure profiles around the propellant tubes that pass through the exit-crossover region.

Two definite flow regimes that are characterized by the calculated value of the local Reynolds number were identified within this region. Various local effects due to geometry were determined. The effect of flow blockage in the concentric flow channel around propellant pressure tubes was measured.

Sufficient data are presented so that the flow conditions in the exit region may be compared with previous semiempirical correlations for heat transfer in similar geometries. The data could also be used to design an experimental heat-transfer apparatus with water flow conditions that would match those existing in the exit region of the full-scale tungsten water-moderated nuclear reactor.

INTRODUCTION

The tungsten water-moderated nuclear reactor (TWMR) concept has been studied at the Lewis Research Center as a possible space-propulsion engine (ref. 1). In this concept, hydrogen propellant is heated as it passes through the core of a heterogeneous nuclear reactor, and the heated gas is then expanded through a nozzle to provide propulsive thrust.



[REDACTED]

The basic components of the core of this system are schematically represented in figure 1. The hydrogen propellant flow path is indicated in this figure by dashed lines and unshaded arrows. The propellant acts as a coolant for the nozzle and the moderating water before it passes through the core and is expanded through the nozzle.

The water-moderator circuit, which is indicated by the solid lines and shaded arrows in figure 1, is illustrated in more detail in figures 2 and 3. Figure 2 is a schematic diagram of the test equipment that was used to study water flow profiles in the TWMR design. The water enters a circumferential manifold from the inlet pipe and then flows into the inlet-crossover plenum. Figure 3 indicates the water path as it passes from the inlet-crossover region into the reactor-core region.

In the core region, the water flow is divided into two components by a flow divider. This flow divider is a concentric tube placed around the pressure tubes that contain the gas flow. Figure 3 illustrates the two components of flow parallel to the pressure tubes. High-velocity flow passes adjacent to the pressure tubes, while low-velocity bulk flow leaves the core region through holes in the exit support plate.

The problems of water flow distribution within the core region of the reactor have been experimentally studied by Fiero, Miller, and Ribble (ref. 2). Flow distribution was successfully tailored in the full-scale reactor mockup, and no apparent problems remain in this region.

Upon leaving the core region, the water moderator enters a plenum through which propellant tubes intersect. This plenum carries the water to the outer ring of the core for recirculation and is henceforth referred to as the exit-crossover region. The bottom tube sheet of the exit-crossover region is exposed to hot nozzle gases and must be thermally protected. This exit-crossover region and the means for its thermal protection are the main areas of interest in this report.

Thermal analysis of the bottom tube sheet indicates that its temperature is primarily dependent on the heat-transfer coefficient on the water side. This water-side coefficient is closely related to the flow conditions that exist in the exit-crossover region. As indicated by Fiero (ref. 2), the flow configuration in this region is quite complex.

Figure 4 is an enlarged illustration of the region where the propellant tubes pass through the exit-crossover region. For pressure tubes located away from the center of the core, the flow distribution around the tubes has a three-dimensional aspect. High-velocity flow leaves the end of the flow divider tube, which extends $1/2$ inch beyond the support plate, in a vertical direction and turns to flow radially outward. A second component passes through the holes in the support plate in the form of a jet. The third flow component is the bulk radial flow in the crossover region that comes from tubes nearer the center of the reactor.

Pressure profiles measured around the periphery of a tube normal to a free stream indicate different flow conditions around the tube (refs. 3 and 4). A similar determina-

tion of flow conditions in the exit-crossover region may be made by pressure measurements.

Determination of local pressure values in the exit-crossover region should provide sufficient information about water flow behavior to design a high-temperature experiment for determining local coefficients of heat transfer on the water side of the exit tube sheet. Such an experiment might consist of a single heated pressure tube surrounded by a set of unheated adjacent tubes to re-create the water flow geometry. A heated plenum would be used to simulate the hot gases. Different radial locations on the outlet tube sheet could be simulated by adjusting water flows to the apparatus and matching local pressure readings with those obtained in the present tests.

SYMBOLS

D	characteristic geometric length used to calculate Reynolds number, in. (cm)
P_θ	local pressure value at azimuthal location θ , lb/in. ² (N/cm ²)
P_∞	pressure in free stream upstream of cylinder, lb/in. ² (N/cm ²)
Δp	pressure difference from reference point, lb/in. ² (N/cm ²)
Re	Reynolds number, $Du\rho/\mu$
u	local velocity, ft/sec (m/sec)
u_∞	free stream velocity, ft/sec (m/sec)
θ	angle from stagnation point, deg
μ	viscosity, (N)(sec)/m ²
ρ	mass density, g/cm ³

FLOW AND PRESSURE PROFILES NEAR CIRCULAR TUBES

The geometrical configuration of the TWMR exit-crossover region studied in the present tests represents a combination of geometries that have previously been investigated.

The most fundamental geometry represented is that of a single circular tube in an infinite free stream. If potential theory is applied, that is, if no friction is assumed, the expression for the local pressure coefficient around a circular tube (ref. 3) can be described as

$$\frac{P_{\theta} - P_{\infty}}{\frac{\rho u_{\infty}^2}{2}} = 1 - 4 \sin^2 \theta \quad (1)$$

This pressure profile and the experimental curves are found in reference 4 and are reproduced in figure 5. At relatively low flows ($Re < \text{approx. } 4 \times 10^5$), the experimental pressure profile is represented by the subcritical curve of figure 5. The flow is prevented from flowing smoothly around the cylinder (as in the ideal frictionless curve) by friction at the tube wall. The flow separates from the cylinder, and a wake is formed behind the cylinder as illustrated in figure 6. In this wake region, the pressure on the back of the tube remains fairly constant.

For higher Reynolds numbers, a critical velocity is reached above which the separation point is forced farther around the tube as shown in figure 6. The pressure profile for the supercritical flow situation is represented by the supercritical curve of figure 5. This type of experimental pressure profile around a cylinder in a free stream is detailed in reference 5. The pressure readings there were taken at 3° intervals, and, thus, the characteristic shapes are readily observed.

A second geometry in the exit region is a bank of tubes in crossflow as found in some heat-exchanger designs. A summary of studies to measure flow patterns photographically and to determine overall friction factors for banks of tubes is presented in reference 6, which also summarizes heat-transfer-coefficient studies for tubes situated within banks. The variation of heat transfer around tubes in a tube bank was measured for a Reynolds number which was lower by an order of magnitude than those in the present tests. At that level, the similarity of the circumferential profile of heat-transfer rate to the pressure profiles shown in figure 5 is striking.

The third geometry that might contribute to flow patterns in the present configuration is that of a jet impinging on a flat plate. If the water emerging through the support plate inside the flow dividers (fig. 4) impinges upon the exit tube sheet, this condition is represented. An experimental study of heat transfer between a jet of water and a plate held normal to the flow has been performed by Smirnov, Verevochkin, and Brdlick (ref. 7). Their data were taken for Reynolds numbers up to 31 000 and would require severe extrapolation to the conditions that are of interest here.

The geometrical configuration that exists in the TWMR exit-crossover region is far more complex than any one of the three geometries mentioned since it includes components of all three. First, the cylinders are arranged in a triangular array with the bulk crossflow expanding radially. In addition, a flow component exists that starts out parallel to the cylinder completely around its circumference and then turns to join the bulk

[REDACTED]

crossflow. Closely parallel jets of fluid from feed holes in the support plate also influence the local flow.

EXPERIMENTAL TEST FACILITY

Test Vessel

After completion of the reactor water-moderator flow test (ref. 2), the experimental equipment was modified for investigation of flow in the exit-crossover region. The flow test equipment is shown schematically in figure 7. The test vessel was designed to simulate the hydraulic characteristics of the reactor moderator system. However, all other components of the test loop were designed for the test conditions and are not simulations of TWMR hardware. A detailed discussion of external loop characteristics is presented by Fiero (ref. 2).


During testing, considerable energy was added to the water by pumping. To guard against excessive temperatures in the loop, a temperature-controlled valve, normally set at 100° F (38° C), permitted continuous discharge of small amounts of hot water once the temperature reached the designated limit. Cold makeup water was simultaneously added by a level-controlled supply valve.

A bypass filter was connected across the pump in series with two regulating valves which set filter flow at approximately 7 percent of full flow. Most components of the test loop, with the exception of the test vessel, were constructed of low carbon steel; therefore, an organic rust inhibitor was added to the water to prevent excessive corrosion. The system was thus kept relatively clean although a fine brown precipitate was observable in the water. There was no evidence of any instrumentation fouling during the tests from this precipitate.

The test vessel itself was constructed of carbon steel, but the internal components were stainless steel and aluminum. The interior of the test vessel is shown schematically in figure 2. The general flow path of the moderator in the vessel starts at the single inlet pipe that feeds the circumferential inlet manifold. Six portholes distribute the water into the inlet-crossover region; from there, it flows up through the core and side reflector regions. The final orificing scheme given in reference 2 was preserved in all the tests so that the mass flow rate around each pressure tube was approximately equal to 3.75 pounds per second (1.7 kg/sec) at the highest flow conditions tested.

The water then passes into the exit-crossover region, the area of interest in this report. The bulk flow in the exit-crossover region is radially outward to the simulated water-cryogenic heat exchanger, from which the fluid passes into the exit manifold and the outlet pipe.

[REDACTED]



The exit end of the test vessel after partial assembly is shown in figure 8. The support plate, the side reflector, and the annulus between the reflector and the pressure vessel are depicted. When the exit-end pressure head is attached, the simulated cryogenic heat-exchanger tubes fit in this annulus. The six sets of five holes inside the circle of bolts are outlets for side-reflector coolant. The large holes in the center are for placement of pressure tubes and their concentric flow dividers. The low-velocity water flowing through the core enters the exit-crossover region through the small holes in the support plate.

The test vessel with the pressure tubes in place is presented in figure 9. The concentric flow dividers can be seen projecting above the support plate as shown in figure 4. Instrumented pressure tubes used in previous tests are also shown with three pressure lines protruding vertically.

The test vessel after final assembly is shown in figure 10. Flexible connections were made from the pressure sensing lines extending through the vessel head to the Barton pressure transmitters behind the test vessel.

Instrumentation

The basic data taken in these tests were the pressure differences between six circumferential taps equally spaced around the pressure tube at a single axial location. The instrumented pressure tube is shown in figure 11. Six pressure lines can be seen extending from the top of the tube. These lines end at 0.035-inch-diameter (0.089-cm-diam) taps at the axial center of the exit-crossover region as indicated in figure 4.

Differential pressures were measured by using one of the six taps on the tube as a reference pressure. In several runs, a single tap on one tube was used as a reference point for a second instrumented tube as well as for the points on the first tube.

A pressure tube instrumented in this manner could be placed in the large holes shown in figure 8 at the instrumented tube locations indicated in figure 12.

Differential pressure transmitters were used to transfer the measured pressure differences to an automatic data recording system. A schematic of a differential pressure transmitter is shown in figure 13. The hand valves were installed to facilitate zero measurement checks. A zero measurement check was made by closing the valve on the low-pressure line and opening the crossover line to equate the pressures on either side of the transmitter.

Bleed solenoid valves were installed in each line to eliminate trapped air in the measurement lines. The lines were purged before each run, and in normal operation the bleed valves were closed.

[REDACTED]

The total flow rate to the test vessel was measured with a calibrated orifice plate in the inlet flow line. Pressure drop across this plate was also fed to a differential pressure transmitter.

The output signal from the pressure transmitters is an air signal that is proportional to the measured hydraulic pressure differential. These signals are converted to digital form by the digital automatic multiple pressure recorder (DAMPR) which is part of the central automatic digital data encoder (CADDE) at Lewis (ref. 8).

Thermocouple voltages from sensors in the water tank and various pump components were converted to digital data by the automatic voltage digitizer (AVD), also part of the CADDE system.

The data digitizers obtain a time interval proportional to the quantity being measured and then count the pulses of a fixed-frequency oscillator during this time interval. The number of counts is then stored on a magnetic tape and later converted into useable output by an IBM 7094 computer program.

TEST RESULTS

Pressure profiles in the exit-crossover region were measured for three different bulk flow velocities that corresponded to approximately full flow conditions and 80 and 60 percent of full flow. Since the flow was practically equalized for each pressure tube, these conditions amounted to 27.5, 22, and 16.5 gallons per minute (0.104, 0.083, and 0.063 m³/min) inside the flow dividers of each pressure tube.

The various test locations for the instrumented pressure tubes included several different geometrical configurations. The various geometries encountered during the test are shown in figure 14. The bulk cross flow was nominally from the vessel centerline to the circumference. The direction of this flow for each test location is indicated.

During the flow distribution studies (ref. 2), it was found necessary to block off certain of the flow-through holes in the outlet support plate. Both the sealed and the open holes in the support plate are indicated in figure 14.

In contrast to the case in which a single tube lies perpendicular to a free stream, the location of neighboring tubes is important in establishing a pressure profile around a tube. The position of adjacent tubes is also indicated in figure 14.

Measurements in the central area of the test vessel (tube 1) were for the most part inconclusive. If the flow distribution is perfectly symmetrical in the test vessel, no crossflow component should exist at the center tube. The only azimuthally varying condition for the center tube is offered by six parallel jets from the holes in the support plate. Some variation around the center tube was observed, but the locations of maximum differences appeared to shift with time. The most sensitive differential pressure

CONFIDENTIAL

transmitters available on the test rig had a full-scale reading of 5 pounds per square inch (3.45 N/cm^2). The scatter in the data measured for the center tube was often ± 0.15 pound per square inch (0.135 N/cm^2), whereas the maximum variation around the tube was 0.6 pound per square inch (0.41 N/cm^2); therefore, little value can be placed on these measurements. It is not known whether this scatter is caused by a swirling condition at the center of the vessel or whether the instrumentation was not sufficiently sensitive to record pressure variations at this location.

For tube 4, there is still considerable scatter in the data points; however, there is a definite crossflow component here, and a definite profile is observable. Figure 15 shows the measured profile for tube 4 with 3.8 pounds per second (1.72 kg/sec) of water passing down the inside of the flow divider of that tube. The angular location plotted runs counterclockwise from the stagnation point. The calculated maximum radial velocity at the axial position of the pressure taps is 7.45 feet per second (2.27 m/sec). The cross bars on the symbols in figure 15 represent the scatter in the data for five consecutive readings approximately 1 minute apart. The zero point on the curve was the reference pressure for the measurements on this tube. Although a solid line has been drawn as a best fit to the average measured points, the scatter in the data is such that a profile could be drawn with separation at approximately 90° and 210° , a supercritical profile as in curve C of figure 5.

All data taken for tube 4, including material not plotted in figure 15, show a certain asymmetry around the 180° point. This leads to the conclusion that the flow is not yet completely uniform around the tube in this region.

Data taken for tubes located farther from the center of the reactor than tube 4 can be fairly well correlated with the characteristic profiles of figure 5. Typical profiles have been shown in figures 16 to 19. The best-fit curves for the data points in many cases anticipate the characteristic profiles of figure 5. However, some tubes were rotated between runs to provide as many as 12 different azimuthal readings. Such data for tube 21, for instance, outline the characteristic profile in reasonable detail.

An attempt was made to correlate the amplitudes of these tube pressure profiles with calculated local velocities. Table I presents the results of calculations of flow conditions around the various tube locations tested. The basis for each of these calculations was the total mass flow per channel as measured by Fiero (ref. 2) in the flow equalization tests. All water flowing down nearer to the reactor centerline than a particular ring was included in the radial flow around the tubes in that ring. As shown in figure 12, some downflow holes in the support plate have been blocked. The local radial flow past a tube includes water from adjacent inboard holes that may be open. In addition, one-half the liquid flow inside the flow divider of a tube is included in the calculation of maximum velocities past that tube.

TABLE I. - FLOW CONDITIONS FOR TUBES TESTED

Ring	Tube	Maximum velocity, u , ft/sec	Velocity head, $\rho u^2/2$, lb/in. ²	Reynolds number	Characteristic pressure difference around tube	
					lb/in. ²	Velocity heads $\rho \frac{u^2}{2} \equiv 1.0 \text{ velocity head}$
2	4	7.45	0.372	0.745×10^5	0.7	1.88
3	6	7.99	0.43	0.799×10^5	0.75	1.74
		10.66	.76	1.066	1.8	2.36
		13.32	1.19	1.332	2.1	1.76
4	10	10.77	0.78	1.077×10^5	1.5	1.92
		14.36	1.38	1.436	2.2	1.59
		17.95	2.16	1.795	3.5	1.62
5	13	14.59	1.43	1.459×10^5	1.3	0.91
		19.45	2.54	1.945	2.7	1.06
		24.31	3.96	2.431	2.8	.71
6	17	18.86	2.39	1.886×10^5	3.2	1.34
		25.15	4.24	2.515	5.7	1.34
		31.44	6.63	3.144	8.3	1.25
6	20	17.71	2.10	1.771×10^5	2.6	1.24
		23.61	3.74	2.361	4.2	1.12
		29.51	5.84	2.951	5.7	.98
7	21	20.88	2.92	2.088×10^5	2.6	0.89
		27.84	5.20	2.784	5.4	1.04
		34.80	8.12	3.480	11.2	1.38
7	24	20.88	2.92	2.088×10^5	4.5	1.54
		27.84	5.20	2.784	7.0	1.35
		34.80	8.12	3.480	12.6	1.55

[REDACTED]

Table I also lists the amplitudes of the measured pressure differences around tubes as a function of the calculated maximum velocity adjacent to that tube. The separation of the maximum pressure and the flat region of the curve around the 180° point was taken as an indicator of the type of profile measured. In figure 5, this pressure difference was about 2 velocity heads for Reynolds numbers below the critical point (curve B) and about 1.3 velocity heads for those above the critical point.

In figure 20, the measured pressure differences between the maximum and the plateau are plotted in velocity heads against calculated Reynolds number for those tubes that have six adjacent tubes. There seem to be two distinct flow regimes, similar to the critical and subcritical regions in figure 5, with the transition occurring at a calculated Reynolds number of about 2×10^5 . Most values of the pressure difference fall around 1.0 and 1.8 velocity heads in the two regimes. The data for tube 13, which are similar to those for tube 16, could be reasonably plotted as either critical or subcritical profiles and probably occurred in a transition regime.

The data from those tubes not completely surrounded by other tubes come closer to data for a single tube as might be expected. The pressure profile around tube 17 shown in figure 17(c) exhibits a much lower back pressure because of the absence of an adjoining tube at the 180° point. The flow still separates well around the tube as characterized by supercritical flow. No explanation is offered for the slight asymmetry around the 180° point.

Tubes 21 and 24 show similar low back pressure although tube 24 has a marked asymmetry of the low pressure points. Figure 14 indicates that the lowest point in the profile of tube 24 corresponds to the corner location of the tube array where there is no adjacent tube.

Flow Tests with Blocked Flow Dividers

Some tests were run with the flow inside the flow dividers blocked off to test the effect on the pressure profile of the downward flow directly next to the walls of the pressure tube. This blockage was achieved with O-rings that fit tightly in the flow-divider passages. During the previous tests run in this facility to test flow distributions within the core, pitot tubes had been mounted to measure flow inside the flow divider of the instrumented pressure tubes. An O-ring was placed in two of these original instrumented tubes, and flow was measured with the pitot tube. No velocity was indicated in the channels that were blocked in this manner, which seemed to confirm that the O-ring successfully blocked flow inside the flow dividers.

However, measurements taken with the concentric flow divider blocked were not completely successful. Data taken in the exit-crossover region indicate that blockage

CONFIDENTIAL

was successful only part of the time. Figure 16 compares profiles measured around tube 6 with and without the concentric flow channel blocked. At low flow (fig. 16(a)), the blockage resulted in higher pressure differences around the tube; however, at higher flows (figs. 16(b) and (c)), the data are not separable. The low flow data indicate that when the concentric flow passes tangential to the pressure taps, the local pressure at the stagnation point due to radial flow is reduced. Figure 18 shows similar data for tube 21. Here the blocking device held up throughout the test, and larger pressure differences were recorded between blocked and unblocked concentric flow. Data for tube 24 (fig. 19) with blocked flow seem to indicate failure of the blocking device because they appear no different from data taken with an unblocked tube.

CONCLUDING REMARKS

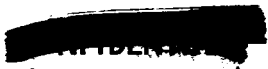
A bank of cylindrical tubes with both concentric flow and crossflow components exhibits pressure-profile characteristics similar to those of a single tube in a free stream. The magnitude of the pressure difference is reduced for a given crossflow rate, but the transition from subcritical to supercritical flow can be observed. The reduction in pressure differences has been experimentally shown to be caused by both the reduction of the stagnation point pressure by the downflow and the increase of backside pressures by the presence of neighboring tubes.

Sufficient information has been obtained about flow configurations in the exit-crossover region of the TWMR so that a heat-transfer simulation rig could be built to measure heat-transfer coefficients.

Lewis Research Center,
National Aeronautics and Space Administration,
Cleveland, Ohio, February 17, 1967,
129-28-02-04-22.

REFERENCES

1. Staff of Lewis Research Center: Nuclear Rocket Propulsion. NASA SP-20, 1962.
2. Fiero, I.; Miller, J. V.; and Ribble, G. H.: Full Scale Water Flow Test of the Tungsten Water-Moderated Nuclear Reactor. NASA TM X-1369.
3. Hunsaker, J. C.; and Rightmire, B. G.: Engineering Applications of Fluid Mechanics. McGraw-Hill Book Co., Inc., 1947.

- 
4. Giedt, Warren H.: Principles of Engineering Heat Transfer. D. Van Nostrand Co., 1957.
 5. Sogin, H. H.; and Subramanian, V. S.: Local Mass Transfer from Circular Cylinders in Cross Flow. J. Heat Transfer, vol. 83, no. 4, Nov. 1961, pp. 483-493.
 6. Knudsen, James G.; and Katz, Donald L.: Fluid Dynamics and Heat Transfer. McGraw-Hill Book Co., Inc., 1958.
 7. Smirnov, V. A.; Verevchkin, G. E.; and Brdlick, P. M.: Heat Transfer between a Jet and a Plate Held Normal to Flow. Int. J. Heat Mass Transfer, vol. 2, no. 1-2, Mar. 1961, pp. 1-7.
 8. Staff of Lewis Laboratory: Central Automatic Data Processing System. NACA TN-4212, 1958.

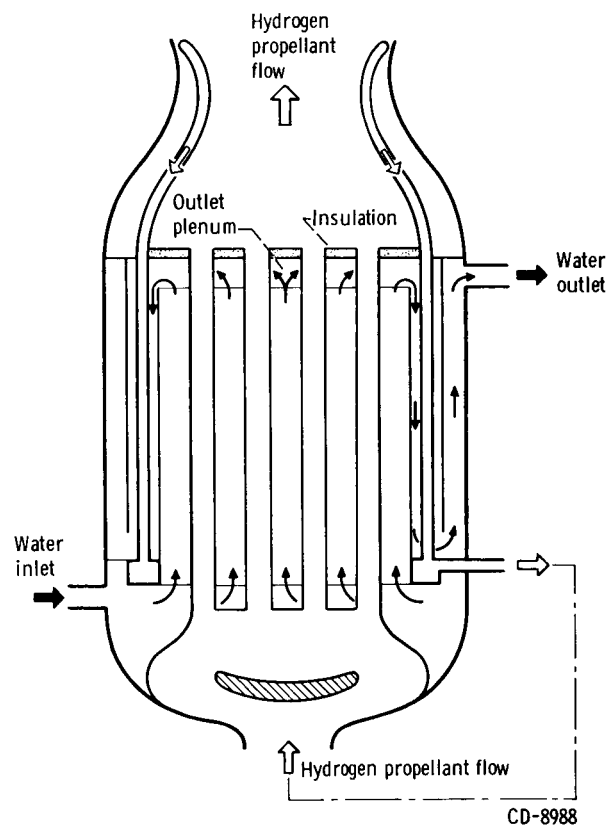


Figure 1. - Schematic diagram of water-moderated rocket reactor.

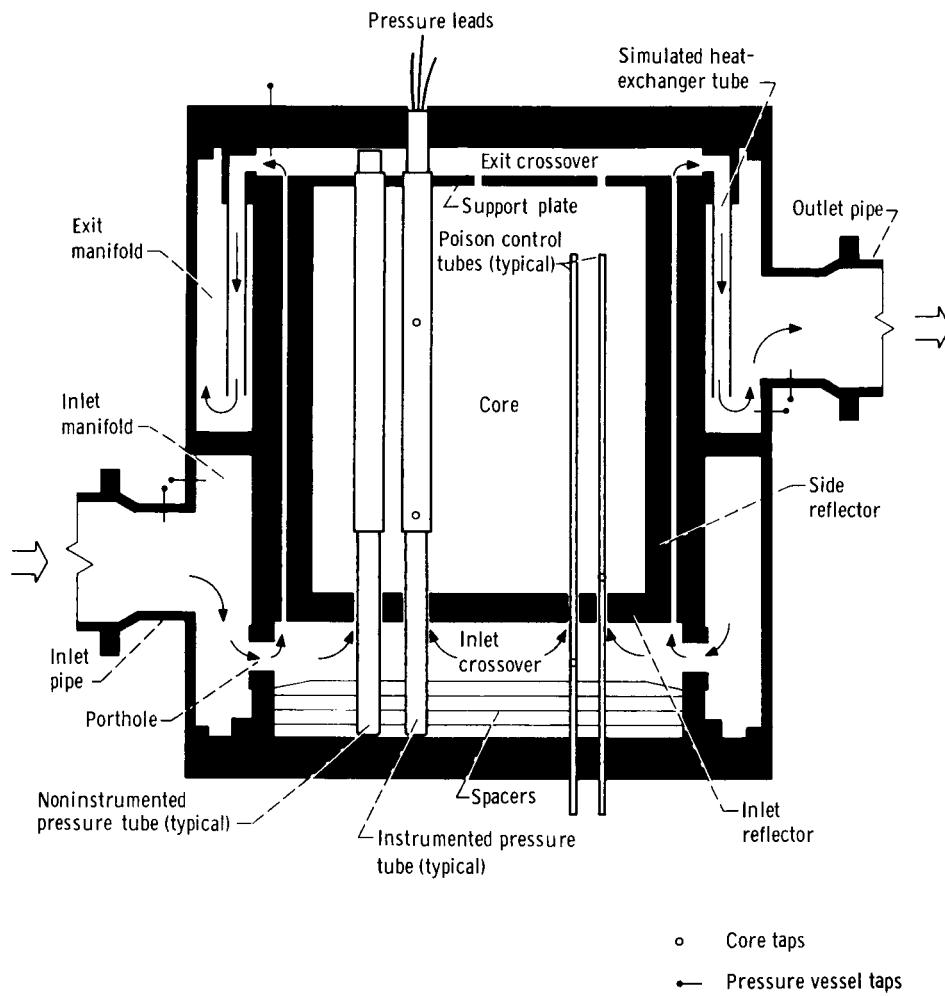


Figure 2. - Schematic diagram of test vessel.

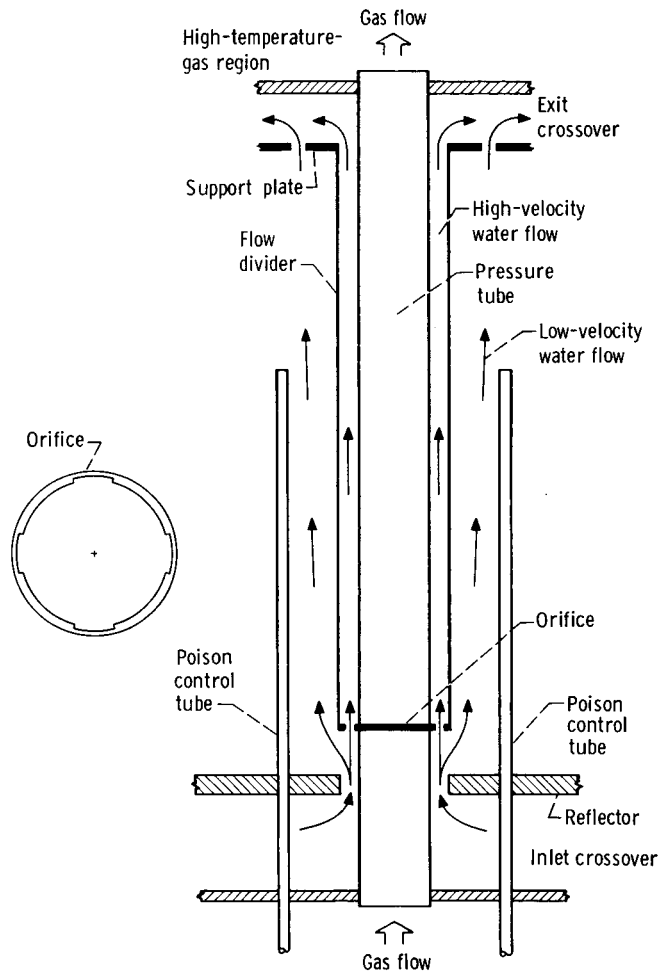


Figure 3. - Schematic diagram of flow from inlet-crossover into reactor core.

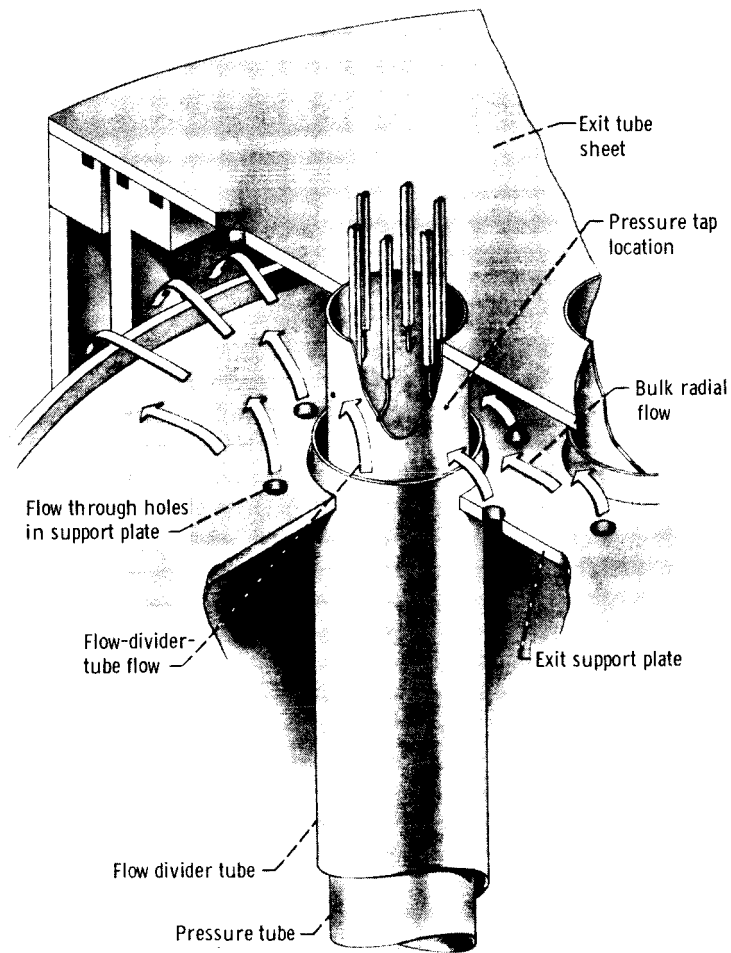


Figure 4. - Enlarged view of exit-crossover region showing tube at outer edge of core.

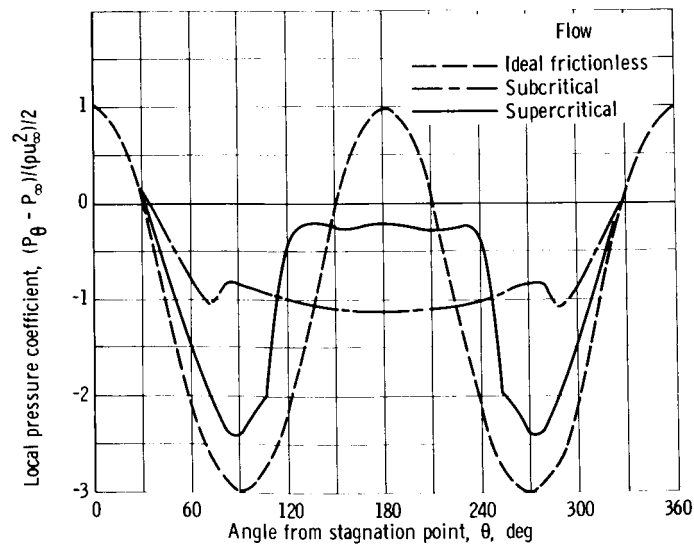
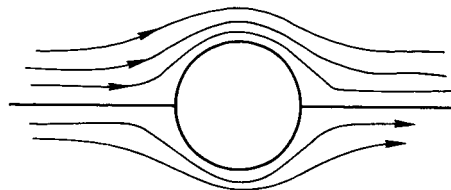
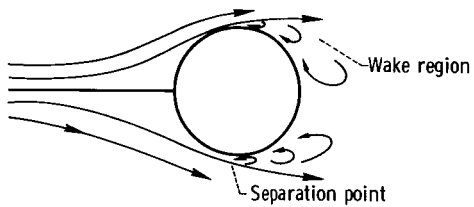


Figure 5. - Pressure profiles around circular tube.

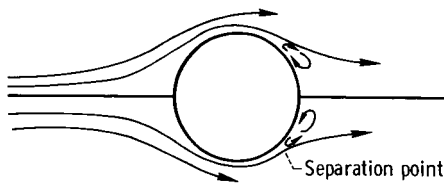
CONFIDENTIAL



(a) Ideal flow.



(b) Subcritical flow.



(c) Supercritical flow.

Figure 6. - Flow around circular tube in free stream.

CONFIDENTIAL

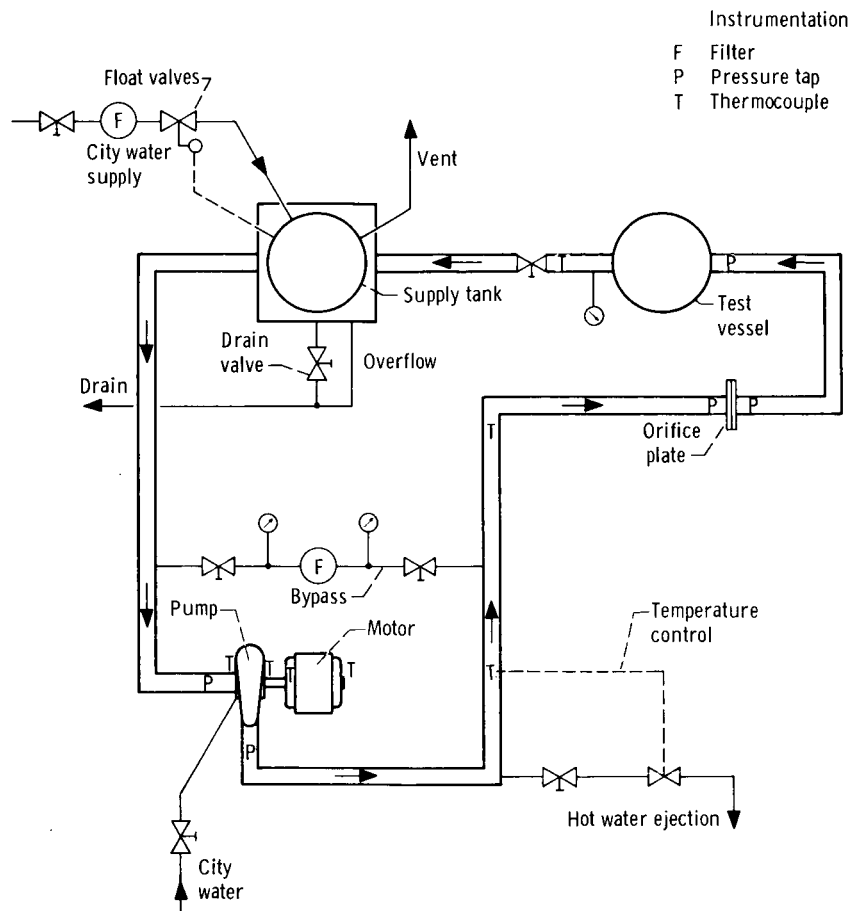


Figure 7. - Schematic diagram of test installation.

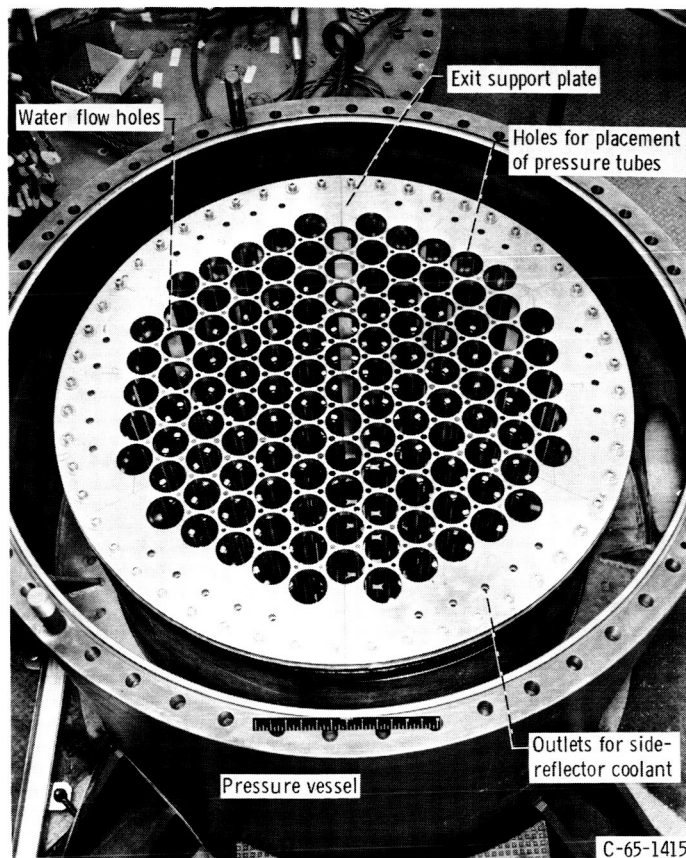


Figure 8. - Exit end of test vessel after partial assembly.

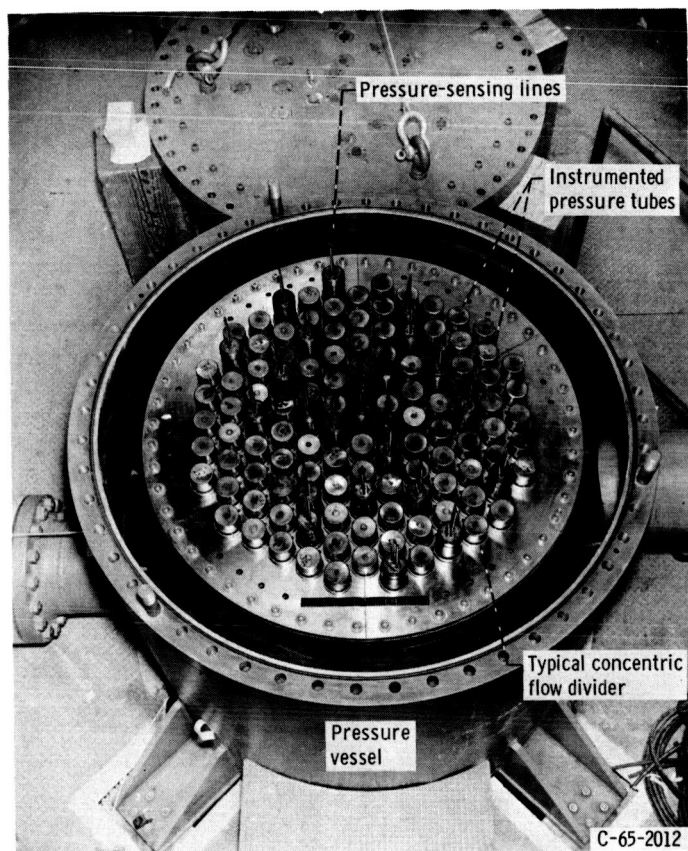


Figure 9. - Test vessel with pressure tubes in place.



Figure 10. - Test vessel after final assembly.

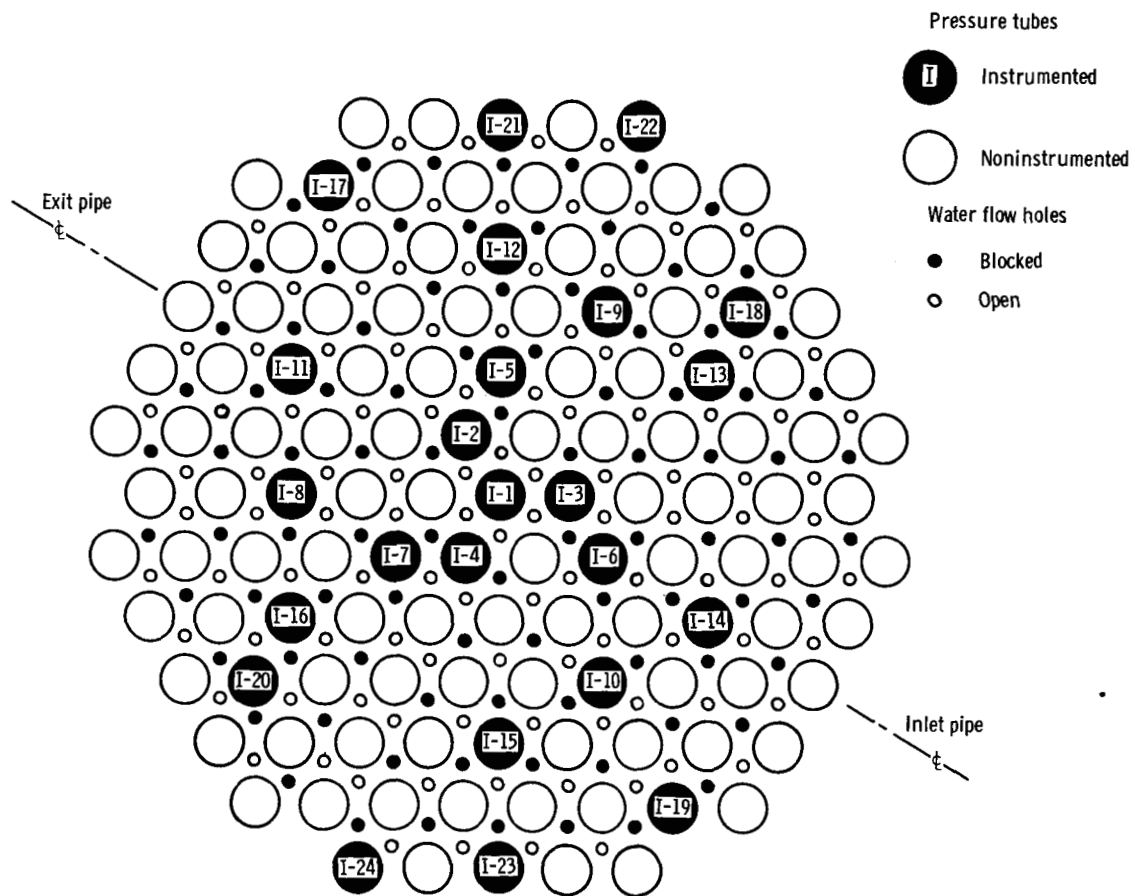
CONFIDENTIAL



C-66-3733

Figure 11. - Instrumented pressure tube.

CONFIDENTIAL



CD-8860

Figure 12. - Pressure tube locations.

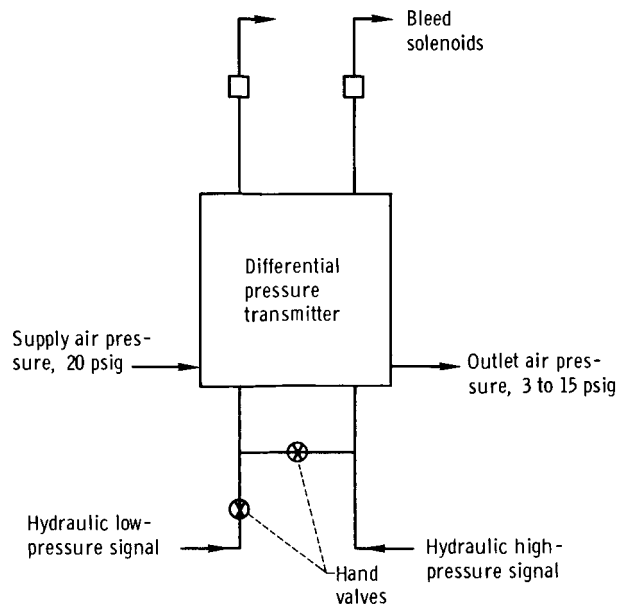


Figure 13. - Schematic of hydraulic-to-pneumatic differential pressure converter and transmitter.

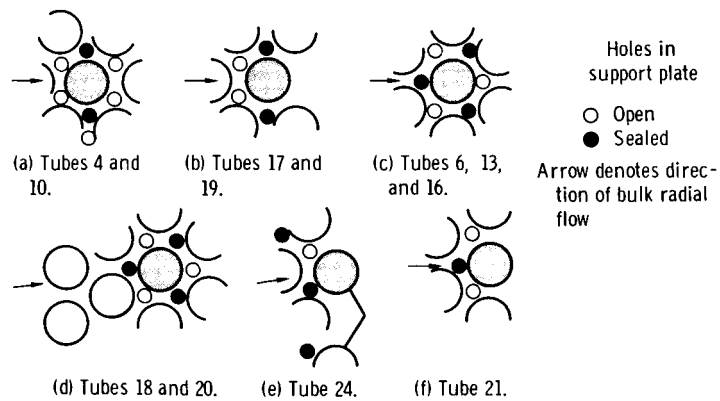


Figure 14. - Geometric configuration of tubes tested.

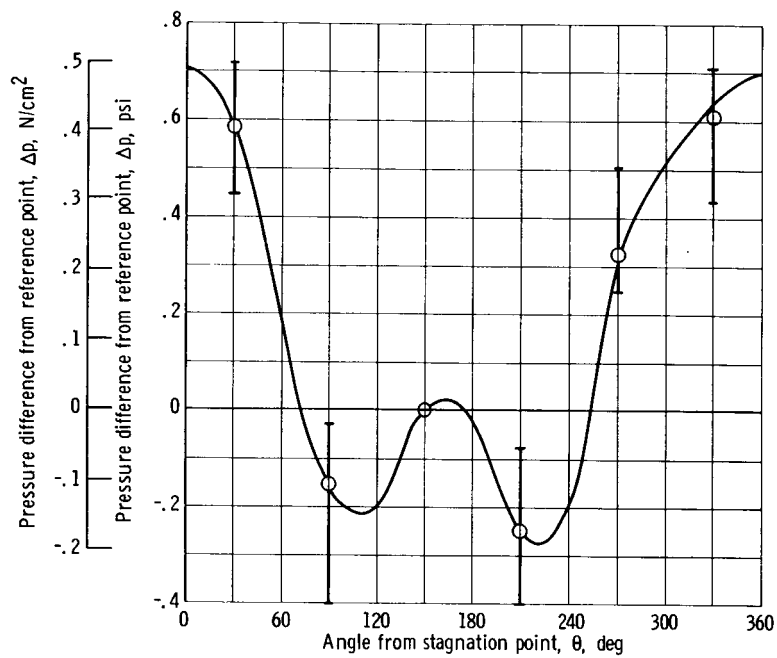


Figure 15. - Pressure profile around tube 4 at full flow. Runs 286 to 290.

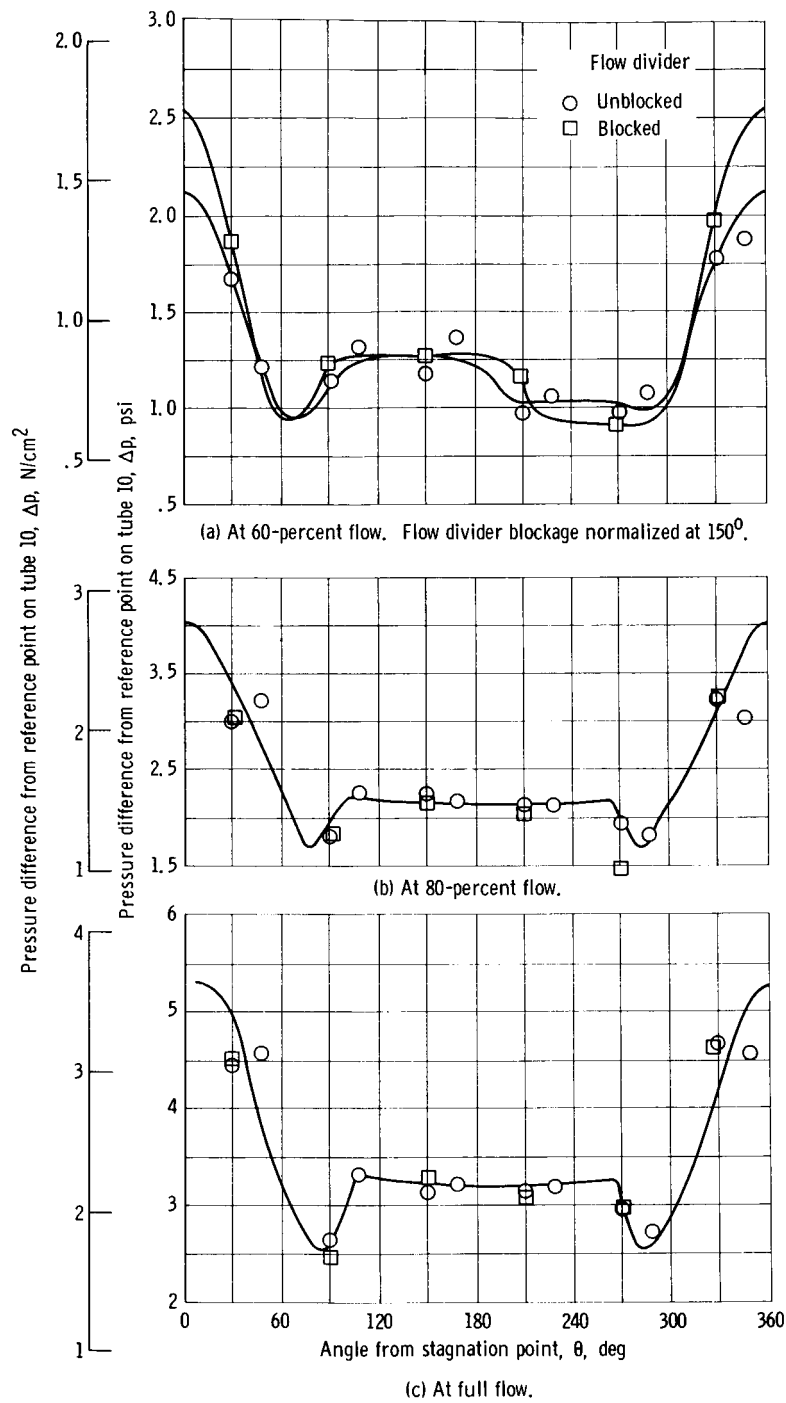


Figure 16. - Pressure profiles around tube 6.

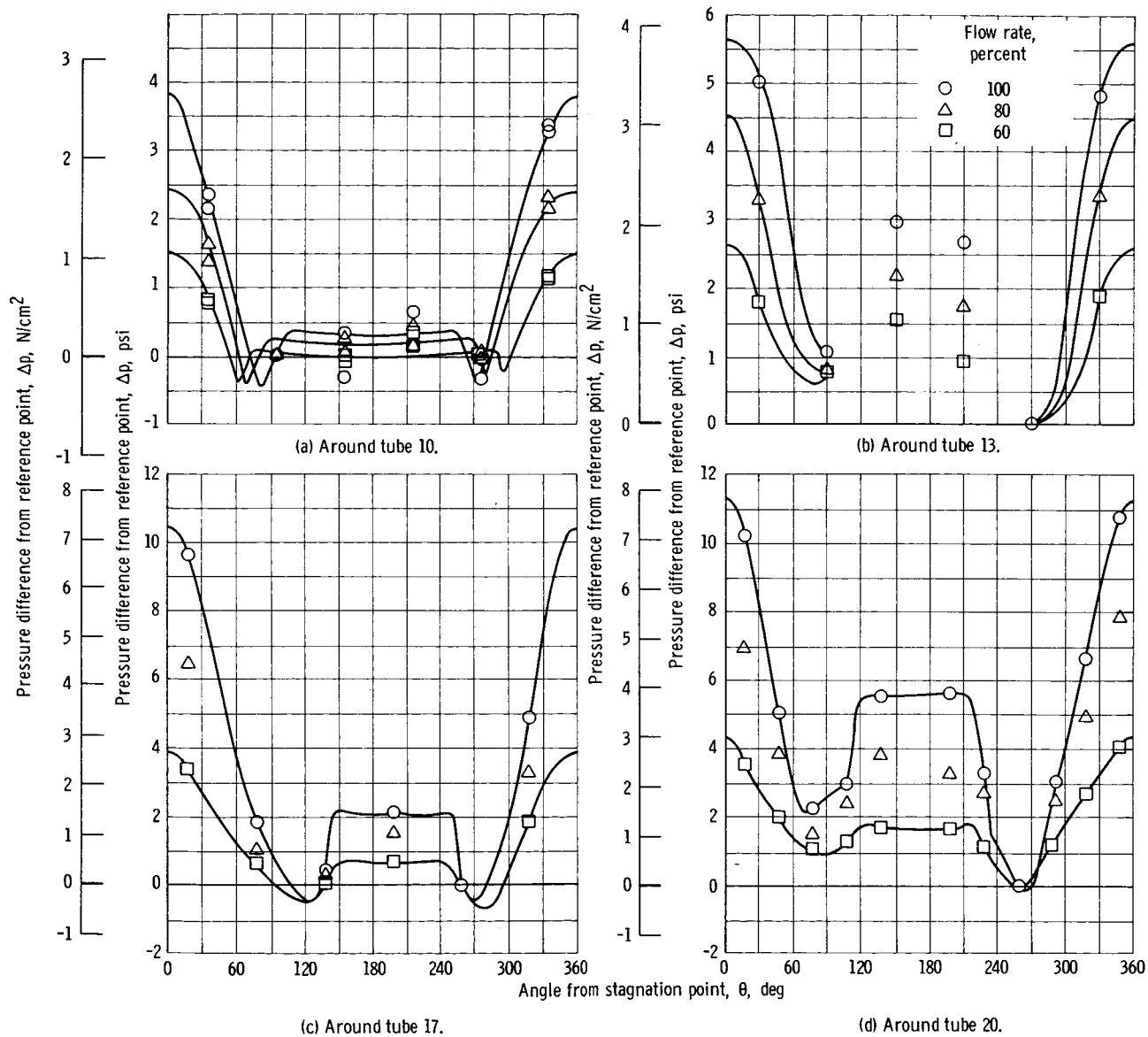


Figure 17. - Pressure profiles.

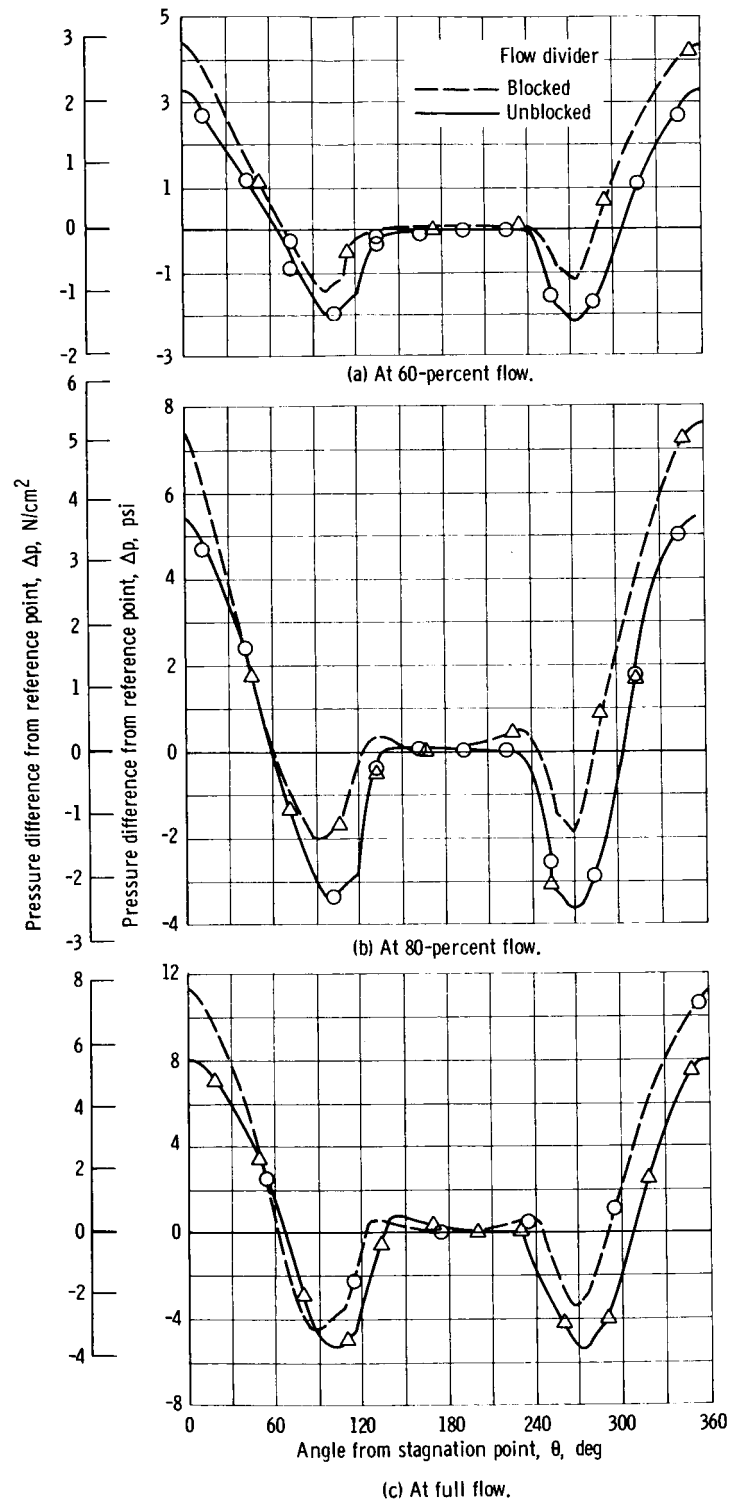


Figure 18. - Pressure profiles around tube 21.

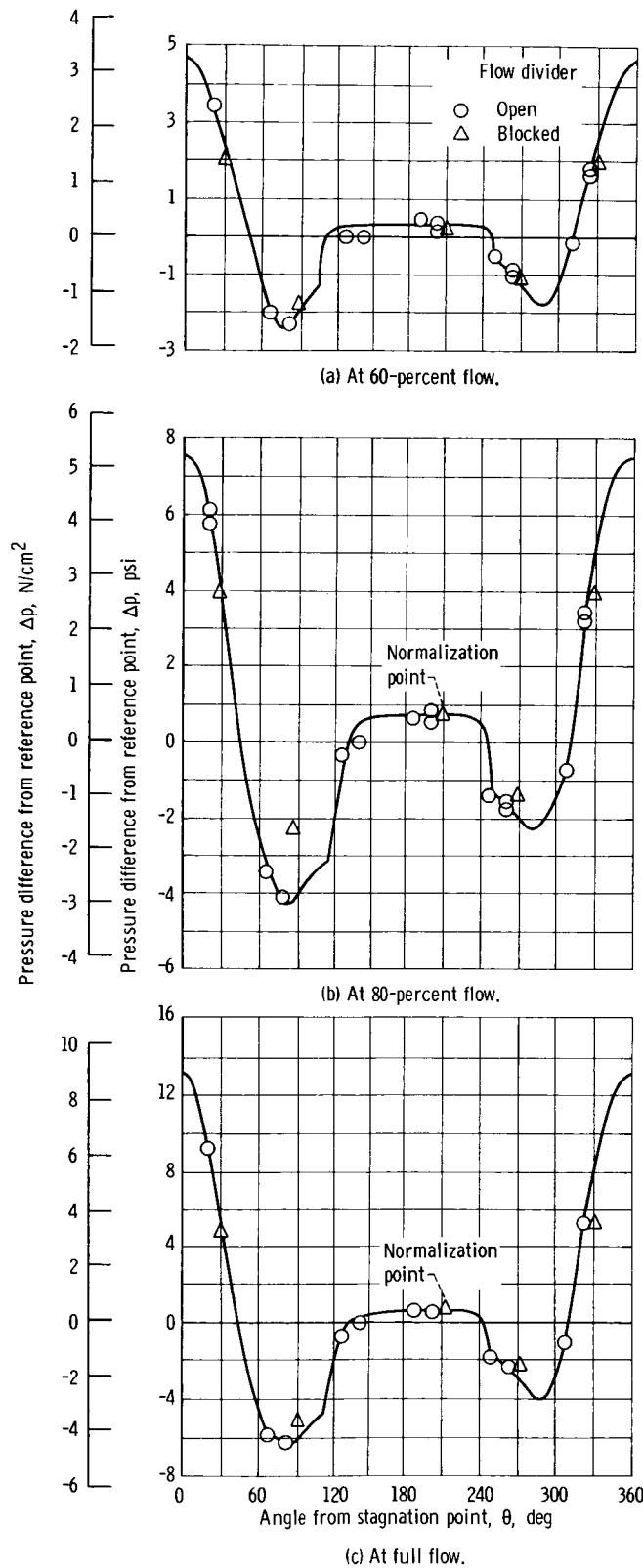


Figure 19. - Pressure profiles around tube 24.

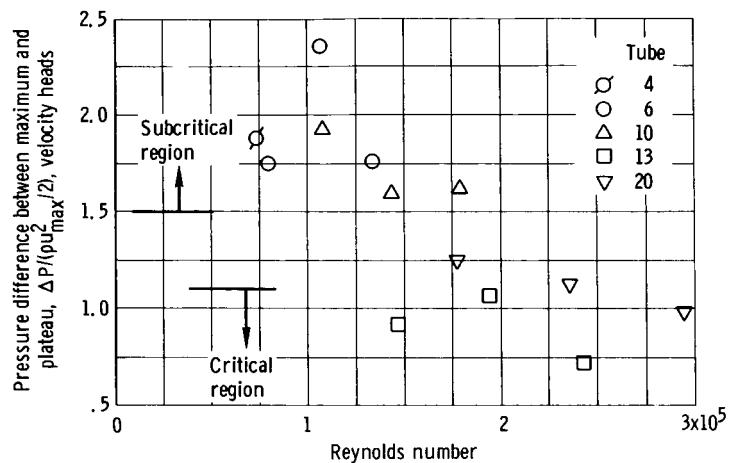


Figure 20. - Flow profile character as function of Reynolds number.

[REDACTED]

"The aeronautical and space activities of the United States shall be conducted so as to contribute . . . to the expansion of human knowledge of phenomena in the atmosphere and space. The Administration shall provide for the widest practicable and appropriate dissemination of information concerning its activities and the results thereof."

—NATIONAL AERONAUTICS AND SPACE ACT OF 1958

NASA SCIENTIFIC AND TECHNICAL PUBLICATIONS

TECHNICAL REPORTS: Scientific and technical information considered important, complete, and a lasting contribution to existing knowledge.

TECHNICAL NOTES: Information less broad in scope but nevertheless of importance as a contribution to existing knowledge.

TECHNICAL MEMORANDUMS: Information receiving limited distribution because of preliminary data, security classification, or other reasons.

CONTRACTOR REPORTS: Scientific and technical information generated under a NASA contract or grant and considered an important contribution to existing knowledge.

TECHNICAL TRANSLATIONS: Information published in a foreign language considered to merit NASA distribution in English.

SPECIAL PUBLICATIONS: Information derived from or of value to NASA activities. Publications include conference proceedings, monographs, data compilations, handbooks, sourcebooks, and special bibliographies.

TECHNOLOGY UTILIZATION PUBLICATIONS: Information on technology used by NASA that may be of particular interest in commercial and other non-aerospace applications. Publications include Tech Briefs, Technology Utilization Reports and Notes, and Technology Surveys.

Details on the availability of these publications may be obtained from:

SCIENTIFIC AND TECHNICAL INFORMATION DIVISION
NATIONAL AERONAUTICS AND SPACE ADMINISTRATION

Washington, D.C. 20546

[REDACTED]